PERGAMON

International Journal of Heat and Mass Transfer 41 (1998) 3121–3129

International Journal of HEAT and MASS TRANSFER

Pulsed-wire technique for velocity measurements in natural convection flows—a numerical optimisation tool

M. Grignon*, E. Mathioulakis, P. Ngae, J. G. Poloniecki

Centre d'Etude de Mécanique d'Ile de France-Groupe de Mécanique des Fluides et Energétique, Université d'Evry Val d'Essonne, 40 rue du Pelvoux, 91020 Evry Cedex, France

Received 1 November 1996; in final form 15 December 1997

Abstract

A computer model for improving the potentialities of the parallel wires anemometers is presented. A new calculation technique has been developed, taking into account the diffusion effects in the transfer phenomena that occur during the measurement procedure. A numerical model which represents the behaviour of a unique wire in relaxation has been developed. It has been shown that, for the range of speeds encountered in natural convection, the phase of relaxation could be separated into two periods. During the first period the diffusion transfer is dominant, whereas in the second period the convection transfer becomes more significant. Moreover, the energy of the emitter wire is introduced as a source term in a transport model built upon the Patankar's method. The validity of the prediction is illustrated by comparison with measurements and very good agreement has been achieved.

Nomenclature

a subscript for the air
A, B, n constants, in the Collis and Williams correlation
C_p, C_w specific heat of the air, of the wire
d wire diameter
g gravitational acceleration
h heat transfer coefficient
I heating current
k, k_w thermal conductivity of the air, of the wire
KE ratio of the heat transfer by a specific mode to the maximal convective exchange
l wire length
Nu Nusselt number hl/k
p pressure
p^* modified pressure $p^* = p + \rho g y$
P_{el} electrical power supplied to the wire during the pulse
r radial coordinate
R electrical resistance of the wire
Re Reynolds number Ul/v
R_m mean value of the electrical resistance of the wire during heating
S heat source
t time
t_M time at the end of heating
T wire temperature, equations (1), (3); flow temperature, equations (11), (12)
$T_a(t)$ local flow temperature for the receiver wire, equation (11)
T_m film temperature
T_M emitter wire temperature at the end of heating
T_∞ air or ambient temperature
T_w wire temperature
$T2_\alpha$ temperature of the receiver wire when α is the value of the angle of the incidence
$T2_{max,0}$ maximum temperature of the receiver wire at null angle of incidence
$\vec{u}$ velocity vector
u, v horizontal and vertical components of the velocity
w subscript for the wire
x, y horizontal and vertical coordinates.

Greek symbols

α angle of incidence (angle between the velocity to be measured and the plane defined by both wires)
β volumetric expansion coefficient
θ $(T-T_\infty)/(T_M-T_\infty)$, dimensionless temperature/emitter wire

* Corresponding author.

0017–9310/98 $19.00
PII: S0017-9310(98)00069-6

θ^* $(T2_\alpha - T_\infty)/(T2_{max,0} - T_\infty)$, dimensionless temperature/ receiver wire
ν kinematic viscosity
ρ, ρ_w density of the air, of the wire
τ time constant.

1. Introduction

The parallel wires anemometer (Fig. 1), of which the experimental investigation has been presented in a previous paper [1], is based on the principle of the transport of a heat tracer. The tracer is induced by a short electrical pulse on an emitter wire and goes downstream to a receiver wire. This kind of anemometer is suitable for the measurement of small air speeds ($<2\ m\ s^{-1}$), like the ones observed in natural convection fields. This technology, which has already been used in 1965 by Bauer [2] for large speeds, satisfies the criteria of simplicity in use and low cost. Therefore, larger number of measurement points can be used, providing a better representation of the observed fields. In addition, this sensor enables intrinsically, the measurement of the local temperature. At the present time, this sensor can only be used for the study of bi-dimensional fields, but the study of the influence of the component parallel to the wires is in progress.

Following the experimental validation of the sensor working principle [3], a model was developed for the improvement of the measurement technique. This model should be able to optimise the choice of the sensor dimensions, to estimate the influence of different factors (especially the ambient temperature) and to accelerate the testing procedures. The suggested model is built on the well known equations of mass, momentum and energy conservation, written on an infinite volume surrounding the two wires. The emitter wire is heated by a very short electrical pulse, thus raising its temperature.

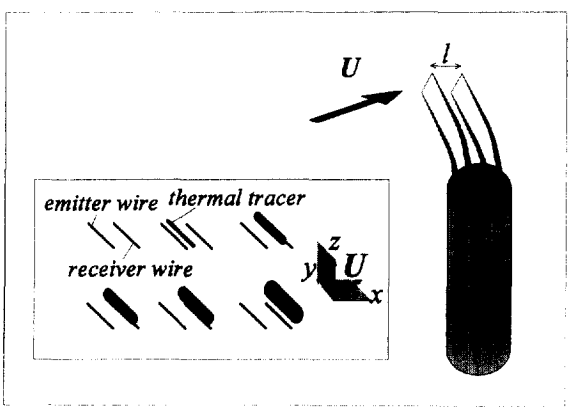

Fig. 1. Parallel wires anemometer—working principle.

At the end of the pulse the relaxation period begins. At this moment, the temperature of the emitter wire begins to decrease, due to the heat exchanges between the air flow. The spot of air leaving the emitter wire is the thermal tracer which changes the temperature of the receiving wire when sweeping it.

The main difficulty, for the numerical modelling, lies in the disparity between the size of the wires and the size of the fluid volume to be discretised. A good representation of the physical phenomena needs either an analytic solution of the problem, or a very thin grid in order to obtain a reliable solution. The analytical solutions introduced by different authors [4, 5] do not describe accurately the behaviour of the emitter wire during the relaxation period (exponential law). On the other hand, a direct numerical simulation requires a very powerful computer, since a huge number of meshes should be used (with 5μm diameter wires and a bi-dimensional spatial domain of a few mm^2, the use of several million meshes grid is necessary).

The proposed numerical solution consists in coupling several models describing the behaviour of the different compounds of the system (emitter wire, space of transportation of the thermal tracer and receiver wire). Each elementary model is based on some hypotheses taking into account the phenomena involved. The final model treats the heat exchanges, considering the two wires as punctual sources. This methodology, applicable to the evaluation of heat transfers between airflows and very thin bodies (not inducing significant modification in the speed field, for low Reynolds numbers), summarises as:

- analysing the thermal exchanges between body and fluid and emitting the laws of a representative model of this;
- calculating independently, for every time step, the values of the thermal flux exchanged between source and fluid by the emitter;
- integrating these values, as a source term in a convection and diffusion model for the whole domain involved in the computation;
- deducing the exchanges between the fluid and the receiver and hence, the evolution of the receiver wire temperature.

2. Modelling the emitter wire

The purpose consists of modelling the behaviour of a wire heated by a pulse of current and cooled by an air flow. A good knowledge of the phenomenon taking place on the emitter wire is necessary to evaluate with precision the temperature variation of the second wire which detects the thermal tracer transported by the flow. This temperature variation should give us information about direction and intensity of the speed of the flow.

2.1. Hypotheses

The model is developed taking into account the following assumptions, proposed by other authors [6, 7], considering that the application range is for velocities lower than 2 ms^{-1}:

- the flow in the vicinity of the wires presents a laminar profile, the diameter of the wires being much more smaller than the smallest scale of turbulence;
- the wire is cooled only by the component of the speed normal to the wire, the aspect ration l/d is accepted as sufficient;
- the overheating being particularly small, the radiative exchanges are negligible;
- at these velocities the frequencies of the fluctuations are around a few hz, and thus, the time constant of the flow is higher than the wire relaxation time; thus, the flow would be considered an isothermal.

2.2. Insufficiencies of a simplified model

The model, commonly associated with a wire of large aspect ratio, and well validated for the high speeds, consists of writing the energy balance on the emitter wire. For this model the energy balance is expressed by:

$$\rho_w \frac{\pi}{4} d^2 l C_w \frac{\partial T}{\partial t} = RI^2 - h\pi dl(T - T_\infty) \tag{1}$$

where I is the heating current ($I \neq 0$ only during the pulse), d the wire diameter, l its length, R its electrical resistance, ρ_w and C_w the density and specific heat of the wire, T and T_∞ the wire and flow temperature, h is the heat exchange evaluated by the relationship proposed by Collis and Williams [8].

Taking into account the relative importance of the exchanged powers and the duration of the pulse (~ 1 μs), the convective exchanged are neglected during the period of heating. Thus, from eq (1), the temperature T_M of the wire at the end of heating at the time t_M can be expressed as follows:

$$T_M = T_\infty + \frac{4R_m I^2}{\pi d^2 l \rho_w C_w} t_M \tag{2}$$

where R_m is the mean value of the electrical resistance of the wire during heating (taking into account the small overheat, this value is obtained in 2 iterations).

In the same manner the relaxation evolution is obtained by integrating the eqn (1) with $I = 0$:

$$T = T_\infty + (T_M - T_\infty)\exp\left(-\frac{t}{\tau}\right) \tag{3}$$

τ is calculated by using the Collis and Williams correlation for low Reynolds numbers airflows [2] ($Re < 44$, $A = 0.24$, $B = 0.56$, $n = 0.45$), so,

$$\tau = \frac{\rho_w d^2 C_w}{4k\left(A + B\left(\frac{Ud}{v}\right)^n\right)}$$

for the speed U, the thermal conductivity k, and the kinematic viscosity v, of the flow being estimated at the mean temperature of the film: $T_M/4 + 3T_\infty/4$ (with $(T_M + T_\infty)/2$ as temperature of the wire).

The comparison between the model computations and the measurements, is made by using the dimensionless temperature θ obtained by the ratio of the wire overheat $(T - T_\infty)$ to the maximum overheat $(T_M - T_\infty)$. The curves presented in Fig. 2 clearly indicate the limits of the model in the case of fast dynamics. The very sharp decrease, at the beginning of the relaxation, shows that this method underestimates the exchanges. The transfers by diffusion toward the air in the vicinity of the wire as well as the losses by the supports need to be rigorously taken into account. Moreover, the resulted curves could not be fitted by an exponential law for the whole relaxation period.

2.2.1. Comparison between the different transfer modes

In order to highlight the relative importance of the different modes of heat transfer taking place on and near the wire, different simulations have been carried out by separating the conduction, the convection and the diffusion. Figure 3 shows the variation of the ratios $KE(t)$ of these transfers to the maximal convective exchange (obtained with the maximal temperature reached just after the pulse):

$$KE(t) = \frac{\text{exchange by a transfer mode at time } t}{\text{maximal convective exchange}}.$$

Although only the qualitative aspect is to be considered (because of the separation of the different transfer modes), Fig. 3 shows that the dominant exchanges at the beginning of the relaxation phase are the diffusive ones. After a short period of time, the convective exchanges

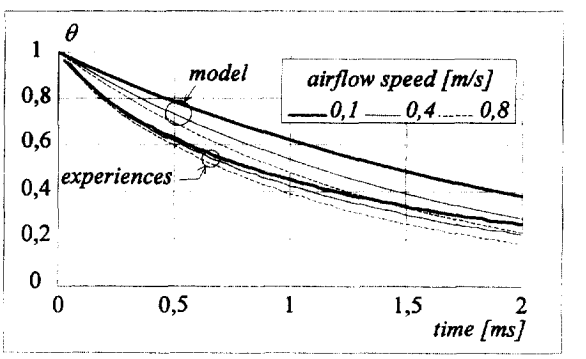

Fig. 2. Comparison between measurements and simplified model.

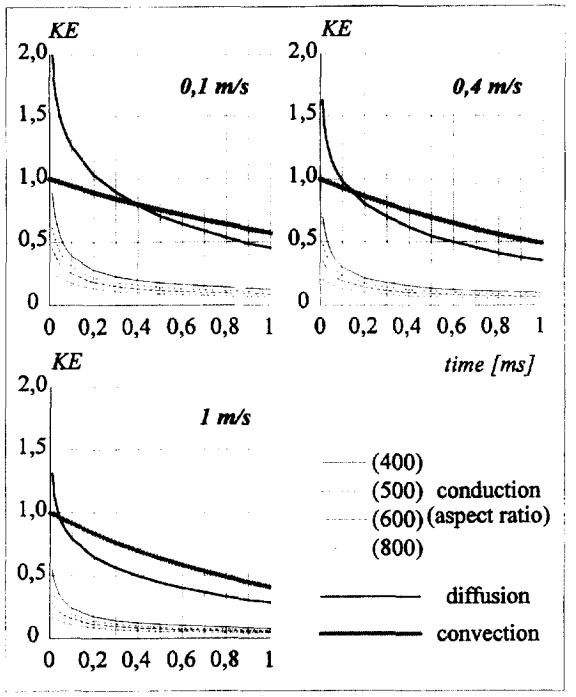

Fig. 3. Ratio between the different modes of thermal transfers—wire of tungsten of diameter 5 μm, overheat temperature after pulse 36 °C.

overcome the other modes of transfers. The figure shows also the influence of the aspect ratio of the wire on the conductive exchanges, and the involvement of this kind of transfer to the cooling of the wire during the first millisecond.

2.3. *The beginning of the relaxation*

During the heating and the first part of the relaxation period, the only exchanges to be taken into account are the conductive ones toward the supports and the conduction-diffusion toward the ambient air. Different mathematical methods could be employed to solve this problem. The numerical method that was finally chosen satisfies the criterion of calculation speed, also allowing the adjustment of the thermophysical characteristics of the fluid according to the air temperature. The duration of heating, despite its brevity, is processed in the same manner. This allows the thermal field in the vicinity of the wire to be determined in a more realistic manner. Furthermore, the wire-ambience discontinuity at the beginning of the relaxation, which generates infinite gradients can be avoided.

2.3.1. *Diffusion in the air*

The emitter wire is considered as a thin body at uniform temperature, on which a very short pulse is applied. Only the exchanges by conduction at the interface between the wire and the air and by diffusion toward the surrounding air are to be considered. The balance of the heat transfer in cylindrical coordinates without longitudinal exchanges, is written as follows:

$$\frac{\rho C_p}{k}\frac{dT_a}{dt} = \frac{1}{r}\frac{dT_a}{dr} + \frac{d^2T_a}{dr^2}, \tag{4}$$

where ρ, C_p and k are the density, the specific heat and the thermal conductivity of the air respectively.

The variation of the internal energy is balanced by the conductive losses to the ambient air (the interface is references by subscript ∞) and by the electrical power P_{el} supplied to the wire during the pulse:

$$\rho_w C_w \frac{l\pi d^2}{4}\frac{dT_w}{dt} = l\pi d\lambda\left(\frac{dT_a}{dr}\right)_{\infty} + P_{el}. \tag{5}$$

where subscripts w and a denote wire and air respectively.

The eqns (4) and (5) are easily integrated on the cylindrical grid but resolution leads to inexact solutions unless the following conditions are fulfilled:

(1) A refined grid which a good representation of the sharp temperature variation in the vicinity of the wire has to be used.
(2) An important volume around the wire has to be considered, since the diffusion effects can be significant far away from the wire (necessity to use a half-infinite domain).
(3) The influence of temperature on the air conductivity should be considered.

In order to satisfy these contradictory conditions, a multi-zone grid was adopted. The grid consists of n concentrical zones (Fig. 4), each of them containing a few meshes with a constant step of space. The steps become progressively larger with the distance to the wire allowing a detailed description of the high gradient area near the wire.

Equations (4) and (5) are discretised using an implicit scheme and solved by a direct method (Gauss–Jordan method). The zones are coupled by considering explicitly the temperature on the interface of the adjacent zones. In order to accelerate the process, each zone is calculated

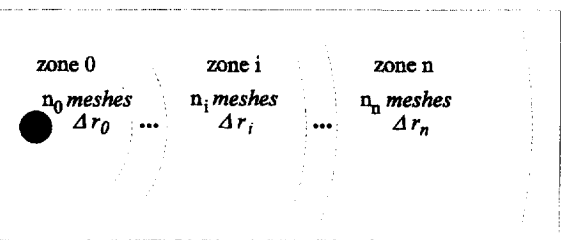

Fig. 4. Multi-zone pattern.

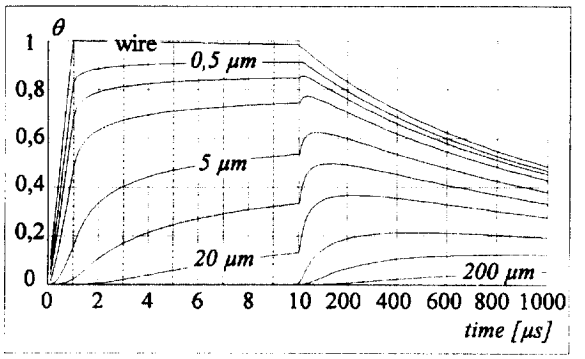

Fig. 5. First phase of the relaxation period—calculation of the diffusion exchanges with a wire of 5 μm diameter. The curves present the temperatures for different distances in the vicinity of the wire.

with its own time step. An example of the results obtained by this model is given in Fig. 5.

2.3.2. Losses through the supports

For the period considered (heating and first phase of the relaxation period) the extra cooling due to the supports should be estimated. The model considers a hot wire tightened between two massive supports and cooled by conduction toward these supports. The temperature of the supports is equal to the ambient temperature. The problem is one-dimensional. The energetic balance equation on an element of wire of length dx (Fig. 6) is:

$$\rho_w C_w \frac{\partial T}{\partial t} = k_w \frac{\partial^2 T}{\partial x^2}. \tag{6}$$

In eqn (6), $T = T_\infty$ (flow temperature), is the boundary condition for the ends of the wire. After discretisation the problem is easily solved by a direct method.

The supports remain at the flow temperature because of their high thermal inertia with respect to the wire.

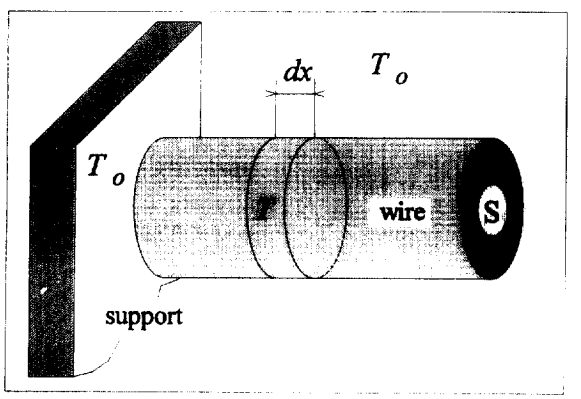

Fig. 6. Scheme of resolution on the wire.

2.3.3. Coupling diffusion—losses through the supports

In order to avoid a more complex model and thus, a large computing time, instead of a three-dimensional model, the conduction in the wire is treated as a corrective term.

The coupling between diffusion and conduction is performed by considering the time constants of the two phenomena. At first the heat exchanged by the wire due to diffusion is calculated and the average wire temperature is determined. Then the conductive losses toward the supports are estimated for a time step equal to the conductive constant time. Finally, the average temperature of the wire is determined.

2.4. Second phase of the relaxation period

For the second stage of the relaxation, a model which realises the coupling of the convection and of the conduction toward the supports is used. Once again, the problem is one-dimensional. As previously, the temperature equation on an element of length dx of wire is obtained by balancing the internal energy variation with the conductive and the convective exchanges. In this case the eqn (6) becomes:

$$\rho_w C_w \frac{\partial T}{\partial t} = \lambda_w \frac{\partial^2 T}{\partial x^2} + \frac{4}{d} h (T_\infty - T), \tag{7}$$

where h is the coefficient of convective exchanges calculated by the correlation of Collis and Williams (with correction of temperature) and estimated at the temperature of local film T_m:

$$Nu \left(\frac{T_m}{T_{ext}} \right)^{-0.17} = 0.24 + 0.56 Re^{0.45}. \tag{8}$$

The variations of the conductivity and the viscosity with respect to the temperature are taken into account by iterative recalculation of the equations coefficients. Supports are considered being at airflow temperature.

2.5. Coupling of the two phases

The transition from the diffusion model to the convection model is realised at the moment when the convection exchanges (calculated for each step of time during the first phase) become higher than the diffusive ones (estimated on the first mesh of the grid by the thermal gradient between the wire and the air). The initial condition for the second phase model is the profile of the wire temperature at the end of the first phase, after the correction due to the conduction towards the supports has been done.

2.5.1. Comparison between measurements and model

As Fig. 7 demonstrates, the proposed model describes the behaviour of the emitter wire during the relaxation

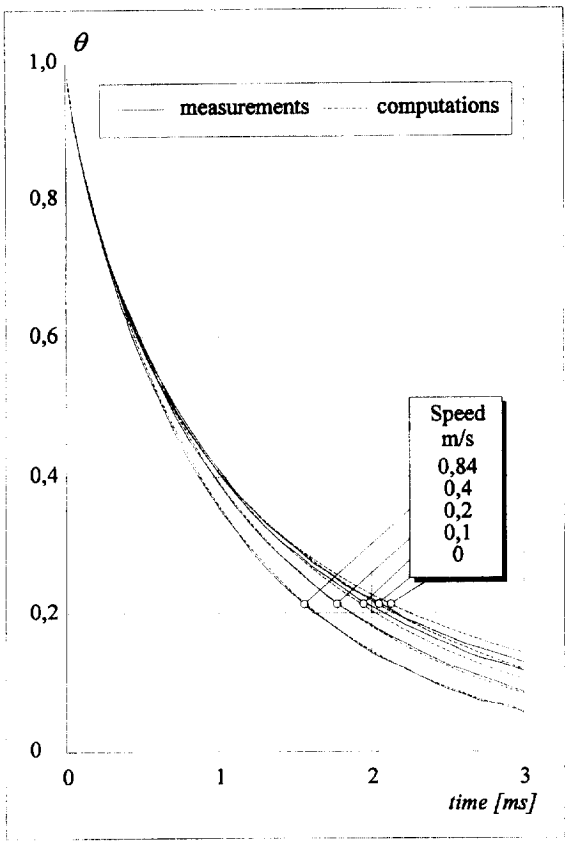

Fig. 7. Relaxation period (diameter of wire: 5.4 μm) —comparison between measurements and model.

period in a satisfactory manner. However some differences appear after 2 ms for the low speeds. Apart from the experimental difficulties (ambient air disturbance, small differences of temperature measurements), it seems that the used correlation noticeably overestimates the exchanges in the case of low speeds and (or) small wire-air temperature differences. Moreover, some adjustments in which the temperature and the Reynolds number are considered, have allowed both sets of curves to be adjusted in a rigorous manner [3].

3. Modelling the receiver wire

The evolution of the temperature on the receiver wire is relatively slow compared to the time constant of the wire. Therefore, it is not necessary to consider the diffusive transfers in the vicinity of the wire. As for the end of the relaxation period, only the convective exchanges (evaluated using the correlation of Collis and Williams) and the conductive losses toward the supports are to be considered. The energy balance, expressed from eqn (7), is still used. In this case, the flow temperature is a local function of time, $T_a(t)$, and actually represents the temperature of the thermal tracer. This equation is numerically solved by using a finite volume method. As an initial condition, the wire is assumed to be at the ambient air temperature T_∞. The same temperature T_∞ is imposed as a boundary condition for the supports, their time constant being large compared with the transition time of the thermal tracer.

4. Transportation of the thermal tracer

The method adopted for the resolution of the equations describing the transport of the thermal tracer (Fig. 8) from the emitter wire toward the receiver wire, is an implicit method based on the SIMPLER algorithm developed by Patankar [9]. The following hypotheses are used:

- The typical scales characterising the system (zone of influence of the a wire and distance separating the two wires) are small with respect to the turbulent scales encountered at the speeds under consideration (smaller than a few meters per second).
- The fluid is Newtonian without sources or sinks of matter.
- The density variation interferes only in the evaluation of buoyancy.

The equations, written for a bi-dimensional domain, are:

Mass balance

$$div\bar{\mathbf{u}} = 0 \tag{9}$$

Momentum balance

horizontal axis x:

$$\frac{\partial}{\partial t}u + \mathrm{div}(\mathbf{u}\cdot u) = -\frac{1}{\rho}\frac{\partial p^*}{\partial x} + v\,\mathrm{div}(\overrightarrow{\mathrm{grad}}\,u) \tag{10}$$

vertical axis y:

$$\frac{\partial}{\partial t}v + \mathrm{div}(\mathbf{u}\cdot v) = -\frac{1}{\rho}\frac{\partial p^*}{\partial y}$$

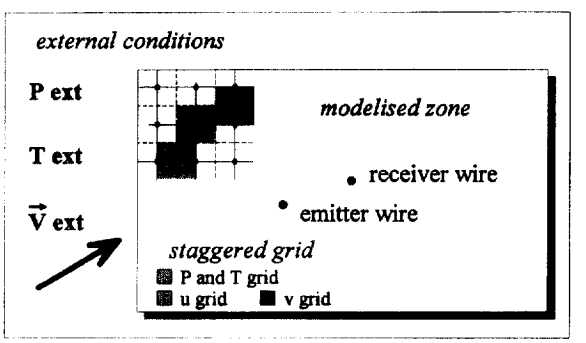

Fig. 8. Modellised space.

$$+v\,\mathrm{div}(\overrightarrow{\mathrm{grad}}\,v)+g\cdot\beta[T-T_a(t)] \quad (11)$$

where $p^* = p+\rho gy$, u and v the components of the local speed $\vec{\mathbf{u}}$

Energy balance:

$$\frac{\partial}{\partial t}T+\mathrm{div}(\mathbf{u}\cdot\mathrm{T}) = \frac{\lambda}{\rho C_p}\mathrm{div}(\overrightarrow{\mathrm{grad}}\,T)+S \quad (12)$$

where S represents the massic heat source.

4.1. Discretisation of the differential equations

4.1.1. The grid

Three staggered grids (Fig. 8), suggested by Harlow and Welch [10], are implemented. The temperatures and the pressures are determined on the first grid, while the x-component of the velocity is calculated on the second grid (the centres of which are on the perpendicular boundary to the x axis of the previous grid). Similarly, a third one is used for the calculation of the y-component of the velocity.

4.1.2. Integration on the grid

The resolution of the above equations is performed by integration on the control volumes and on the time step using the Power-Law Scheme of integration suggested by Patankar [9]. A condition of null gradient on domain's boundaries is adopted for the different variables.

4.2. Source terms and final model

The source term in the final model is actually the one calculated by the previously presented wire model. Thus, the heat flow received or lost by the fluid from the wires is directly integrated in this transport model at every time step. The source term for the emitter wire is extracted from a file, already computed, which contains the average power-values for each time step. For the receiver wire the exchanges are directly computed during the computation marching.

5. Results

5.1. Introduction

The model computations has been compared with measurements obtained by a parallel wires anemometer of 3.5 mm in length and 0.5 mm spacing between the wires. The other main parameters of the experiment were: pulse duration 1 μs, T_M around 66°C, T_z around 20°C. The details of the experimental settings are shown in a previous paper [11].

The dimensionless variable

$$\theta^* = \frac{T2_x - T_z}{T2_{max,0} - T_z}$$

is used for the comparisons. This variable expresses the temperature difference between the ambience (T_z) and the receiver wire ($T2_x$), for an angle of incidence α (Fig. 9) between the plane of the two wires and the direction of the speed, divided by the maximum difference ($T2_{max,0}$) for a null incidence.

5.2. Response of the anemometer as a function of the speed

Figure 10 presents the evolution of the receiver wire dimensionless temperature while it is sweeping by the thermal tracer at small angle incidence. The comparison between model and experimence shows a good agreement between both sets of values.

For the plotting of the calibration curve, the time at which maximum temperature appears on the receiver wire is considered as the output of the anemometer (Fig. 11). The comparison between measurements and computations shows a dispersion smaller than 2%.

5.3. Response of the anemometer as a function of the angle of incidence

The variation of the angle between the airflow and the plane containing the two parallel wires (Fig. 12) highlights two important points:

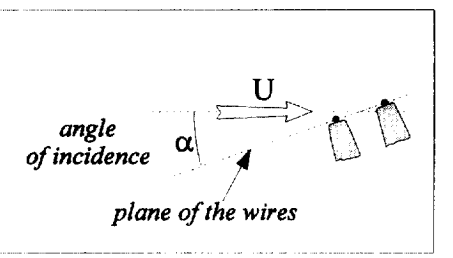

Fig. 9. Angle of incidence.

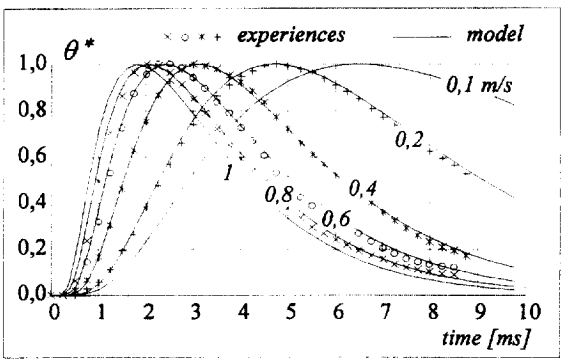

Fig. 10. Temperature evolution of the receiver wire versus the time, for different speeds, comparison measures — model, emitter and receiver wires of 5.4 μm diameter and 3.5 mm in length: spacing: 0.5 mm; pulse: 0.9 A/1 μs.

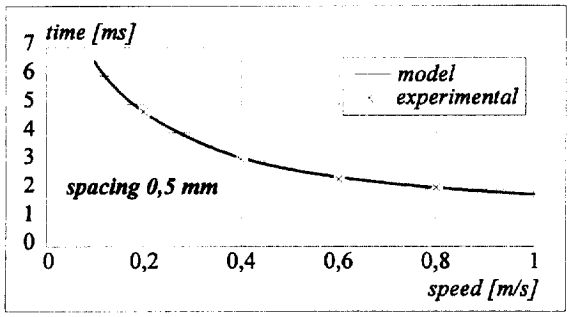

Fig. 11. Interval between the pulse and the appearance of the maximal temperature on the receiver versus the velocity.

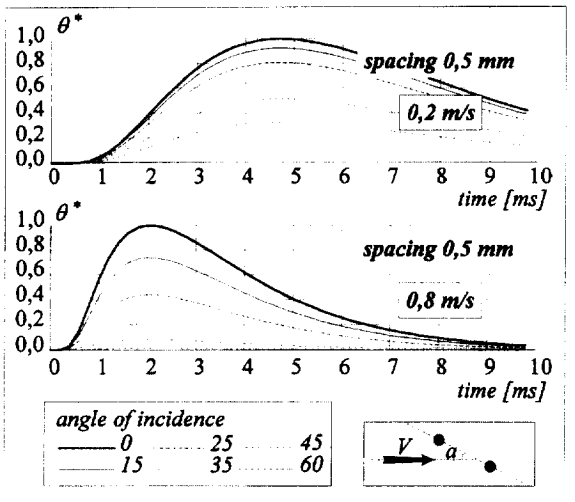

Fig. 12. Response of the receiver wire for different angles of incidence.

- The incidence angle have no influence on the response of the anemometer, since the maximum of temperature appears at the same time.
- The value of this maximum is a function of the incidence angle.

Thus, the velocity can be determined from the time interval between the pulse and the appearance of the maximum on the receiver wire, while the value of this maximum leads to the determination of the velocity direction.

The model, like the measurements, shows a good sensitivity of the sensor in the case of large incidence angles. However a comparison between the model and the measurements shows a dispersion (Fig. 13), related to the sensor geometry (uncertainties on the length of the supports) and to the quality of the ambience around the calibration apparatus for these low speeds [3].

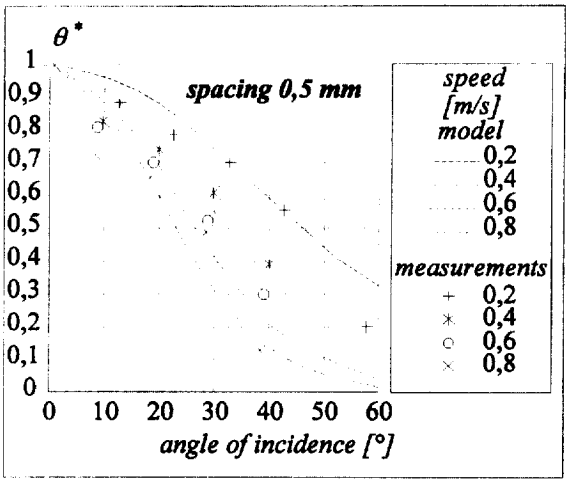

Fig. 13. Values of the maxima—differences between the measurements and the model for different angles of incidence.

5.4. Sensor's optimisation

The model was used for the determination of the influence of the distance between the two wires on the receiver response. Only computations for two values of the distance, corresponding to the limits of the useful interval, are presented here.

The evolution of the temperature for both distances and for different angles of incidence have been shown in Fig. 14. This figure shows clearly that, whatever the spacing is, the maximum of temperature appears at the same instant for different angles of incidence. The analysis of these curves leads in two remarks, the first regarding

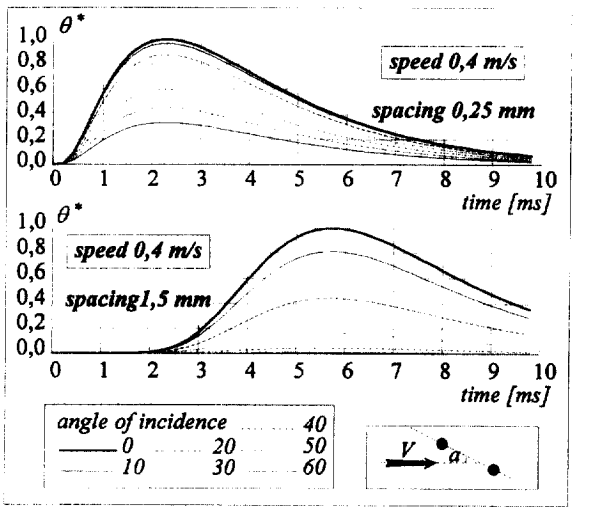

Fig. 14. Influence of wire spacing.

the material aspect, the second regarding the modelling aspect:

- When the wire spacing is small, the capacity of the anemometer to detect large angles of incidence increases.
- Some questions persist about the ability of the model to treat large spacings (commensurable with the length of the wire), owing to the three-dimensionality of the diffusion phenomenon.

6. Conclusion

The presented methodology permits to build an efficient model for our anemometer. The same method may be extended to all thin bodies, characterised by large variations in the spatial scales. In such cases, the contribution of each transfer mode must be rigorously taken into account.

The model is built on a rigorous calculation of the heat flow exchanged by the wires, followed by the integration of the calculated values (source terms) in a general convection–diffusion model. It appropriately describes the behaviour of the parallel wires sensor presented in this paper. It allows the predication with a fine precision of the response curve of the receiver wire for incidences and spacings consistent with the physical characteristics of the system.

This type of parallel wires anemometer could respond, with minimal cost, to the expectations of users confronted with low speeds measurements in two-dimensional airflows. The presented system can be used at the sampling frequencies up to 50 Hz, according to its time constant (around 10 ms). The proposed model allows to improve the development of this kind of sensor and its adaptation to particular problems.

References

[1] Bauer BA. Direct measurement of velocity by hot-wire anemometry. AIAA J. 1965;3(6):1189–91.
[2] Bradbury LJS, Castro IP. A pulsed-wire technique for velocity measurements in highly turbulent flows. J. Fluid Mech 1971;49(4):657–91.
[3] Breton JL. Dissipation thermique de fils chauds soumis à des impulsions calorifiques. Ph.D thesis. Université Paul Sabatier, Toulouse, 1972.
[4] Comte-Bellot G. Anémométrie è fil chaud, cas des fluides incompressibles. Cycle de conférences sur les techniques de mesure dans les écoulements, EDF GDF, Ermenonville, 1973, p. 117–98.
[5] Corrsin S. Turbulence: experimental methods. In: S Flugge editor. Encylopedia of Physics, Fluid Dynamics II, Vol. VIII/2. Springer-Verlag, Berlin, p. 555–89.
[6] Collis DC, Williams MJ. Two-dimensional convection from heated wires at low Reynolds numbers. J. Fluid Mech 1959;6:357–84.
[7] Grignon M. Interactions thermiques entre deux fils fins chauffés et placés dans un écoulement d'air—application à la mesure des faibles vitesses. Ph.D. thesis, Université d'Evry Val d'Essonne, Evry, 1994.
[8] Mathioulakis E, Grignon M. Thermoanémométrie à fils parallèles en régime impulsionnel—étalonnage aux faibles vitesses. Journée d'étude de la SFT, Paris, 1993.
[9] Patankar SV. Numerical heat transfer and fluid flow. Hemisphere,New York, 1980.
[10] Harlow FH, Welch JE. Numerical simulation of time-dependent viscous incompressible flow of fluid with a free surface. Phys Fluids 1965;8:2182–9.
[11] Mathioulakis E, Grignon M, Poloniecki JG. A pulsed-wire technique for velocity and temperature measurements in natural convection flows. Exp in Fluids 1994;18:82–6.